ORIGINAL RESEARCH PAPER

A Spectroscopic Mechanism for Primary Olfactory Reception

Luca Turin

Department of Anatomy and Developmental Biology, University College London, Gower Street, London WC1E 6BT, UK

Correspondence to be sent to: Luca Turin, Department of Anatomy and Developmental Biology, University College London, Gower Street, London WC1E 6BT, UK

Abstract

A novel theory of primary olfactory reception is described. It proposes that olfactory receptors respond not to the shape of the molecules but to their vibrations. It differs from previous vibrational theories (Dyson, Wright) in providing a detailed and plausible mechanism for biological transduction of molecular vibrations: inelastic electron tunnelling. Elements of the tunnelling spectroscope are identified in putative olfactory receptors and their associated G-protein. Means of calculating electron tunnelling spectra of odorant molecules are described. Several examples are given of correlations between tunnelling spectrum and odour in structurally unrelated molecules. As predicted, molecules of very similar shape but differing in vibrations smell different. The most striking instance is that of pure acetophenone and its fully deuterated analogue acetophenone-d_8, which smell different despite being identical in structure. This fact cannot, it seems, be explained by structure-based theories of odour. The evidence presented here suggests instead that olfaction, like colour vision and hearing, is a spectral sense. **Chem. Senses 21: 773–791, 1996.**

Introduction

Putative olfactory receptors have been identified previously (Buck and Axel, 1991; Buck, 1993; Ngai *et al.*, 1993; Raming *et al.*, 1993). Signal transduction is known to involve a G-protein-coupled adenylate cyclase mechanism (for review see Shepherd, 1994). However, the mechanism by which receptors detect odorants, and thus the molecular basis of odour, remain unclear. As has been repeatedly pointed out, structure–odour relations provide conflicting evidence (Beets, 1971, 1978; Klopping, 1971; Ohloff, 1986; Weyerstahl, 1994). On the one hand, molecules of widely different structures can have similar odours, e.g. the bitter almond character, shared by as many as 75 molecules, including the triatomic molecule HCN. On the other hand, minor changes to the structure of a molecule can alter its smell character completely. For example, isomers such as vanillin (3-methoxy-4-hydroxy-benzaldehyde) and isovanillin (3-hydroxy-4-methoxybenz-aldehyde), and enantiomers such as R- and S-carvone smell very different (Arctander,

1994). Furthermore, olfaction is often 'analytical': the presence in a molecule of certain chemical groups such as aldehydes, carbonyls, nitriles, isothiocyanates, thiols, esters and ethers is frequently correlated with a particular odour. The example best known to non-specialists is thiol (SH), which gives any odorant molecule a unique 'sulphuraceous' (rotten egg, garlic) odour character. Structure–odour theories tend to reflect one or the other line of evidence: 'functional group' theories emphasize the analytical view, but do not provide a mechanism by which individual groups can be detected regardless of molecular shape. Theories based exclusively on shape enjoy some success within specific odorant groups, but do not account for the striking chemical group regularities. Nor do they account for the fact that very different structures give similar odours.

The present work originates from a theory first put forward by Dyson (1938). He suggested that olfactory organs might somehow detect molecular vibrations. If the whole vibrational range to 4000 cm^{-1} were detected as by a Raman or IR spectroscope, detection of functional groups would be explained, since many have distinctive vibrational signatures, usually above 1000 cm^{-1}. This theory was modified in a series of articles by Wright and co-workers (Wright, 1977 and references therein). They argued that since optical means were out of the question, detection of molecular vibrations must necessarily be mechanical in nature, and therefore only vibrational modes excited at body temperature could be detected. This meant that the range of detectable vibrations must lie below ~2 kT, or 500 cm^{-1}. Correlations between spectrum and odour in that range were reported, but they were achieved by dismissing discrepant peaks as 'anosmic', and adding some at computed 'difference' frequencies. In any event, it was always clear that the region below 500 cm^{-1} could not determine odour (Klopping 1971): many inorganic molecules with strong, distinctive odours, such as NH_3, H_2S, O_3 and HCN, vibrate only in the range 700–3500 cm^{-1}. Furthermore, the basic idea of vibrational spectroscopy could never account for the different odours of enantiomers. Lastly, no plausible mechanism was ever found by which a biological system could perform vibrational spectroscopy by mechanical means, and the theory eventually fell from favour.

This article will cover the following topics: inelastic electron tunnelling spectroscopy; its implementation in olfactory receptors; evidence from neurophysiology; the calculation of structure–odour relations; the problem of odourless molecules; applications of the theory to a few selected structure–odour problems; and isotope replacement.

A biological 'spectroscope'

Inelastic electron tunnelling spectroscopy (IETS) is a non-optical form of vibrational spectroscopy (Jaklevic and Lambe, 1966; Hansma, 1982; Adkins and Phillips, 1985). It relies on the interaction between electrons tunnelling across a narrow gap between metallic electrodes and a molecule in the gap. When the gap is empty, tunnelling electrons cross the gap at constant energy and the tunnelling current is proportional to the overlap between filled and empty electronic states in the metals. Thus, if the density of filled and empty states is constant, the junction is ohmic. If a molecule is present in the gap, tunnelling electrons will be scattered by the partial charges on the molecule's

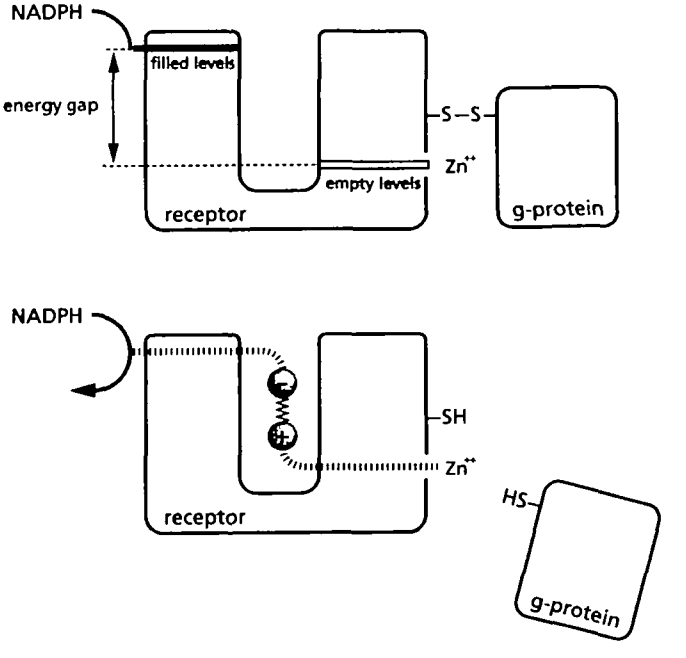

Figure 1 Schematic of the proposed transduction mechanism: the receptor protein accepts electrons from a soluble electron donor (NADPH). When the receptor binding site is empty (top), electrons are unable to tunnel across the binding site because no empty levels are available at the appropriate energy. The disulphide bridge between the receptor and its associated G-protein remains in the oxidized state. When an odorant (here represented as an elastic dipole) occupies the binding site (bottom), electrons can lose energy during tunnelling by exciting its vibrational mode. This only happens if the energy of the vibrational mode equals the energy gap between the filled and empty levels. Electrons then flow through the protein and reduce the disulphide bridge via a zinc ion, thus releasing the G-protein for further transduction steps.

constituent atoms, and lose energy to the molecule by exciting one of its vibrational modes. When this happens, electrons can follow an indirect path, first exciting the molecular vibration and then tunnelling to the second metal at a lower energy. The new tunnelling path causes an increase in the conductance of the junction. Successive vibrational modes are excited as junction voltage is increased. Differentiating the current–voltage relationship twice yields narrow peaks at energies corresponding to those of the vibrational modes of the molecule in the gap.

Metallic conductors are absent in biology, but electron transfer is ubiquitous. Doing IETS with proteins (Figure 1) would involve addition and removal of electrons at well-defined energy levels on either side of an odorant-sized (<400 daltons) binding site which serves as the tunnelling gap. On one side of the gap a donor site with occupied donor levels is present, while an acceptor site with empty acceptor levels is on the other side. If there is nothing between the electron source (donor) and sink (acceptor), then for direct tunnelling to occur there must be an (occupied) energy level in the source which matches the energy of an (empty) state in the sink.

If there is a molecule between the electron source and electron sink, and if that molecule vibrates, then (taking the energy of the vibrational quantum as E) indirect tunnelling can occur by an additional channel if there is an energy level in the source with energy E above that in the sink. After tunnelling, the molecule will have a vibrational energy higher by E. In other words, tunnelling occurs only when a molecular vibrational energy E matches the energy difference between the energy level of the donor and the energy level of the acceptor. The receptor then operates as a spectrometer which allows it to detect a single well-defined energy, E. If the change in energy between donor and acceptor levels is sufficiently large, tunnelling current flows across the device only when a molecule with the appropriate vibrational energy is present in the gap. If there are several vibrational modes, which one(s) will get excited will depend on the relative strengths of the coupling, and that may be expected to depend, among other things, on the partial charges on the atoms and the relative orientation of the charge movements with respect to the electron tunnelling path.

Unlike conventional IETS, 'biological IETS' does not involve scanning of the energy range, which would probably be unfeasible in a biological system. Instead, the range of vibrational energies is covered piecewise by a series of receptors tuned to different energies. The energy range is limited only by the e.m.f. (reducing power) of the electron source. An estimate of biological reducing power is 500 mV (1 eV = 8086 cm^{-1}) (Fraùsto da Silva and Williams, 1993), which means that the entire vibrational range to 4000 cm^{-1} could be sampled. To cover the vibrational spectrum, several receptor classes would be required, each tuned to a different segment of the vibrational spectrum. A small number might be sufficient, much as three pigments with broad, partially overlapping absorption spectra suffice for colour vision. One essential feature of the biological spectrometer is its relatively poor resolution. Vibronic coupling, which results in a broadening of acceptor and donor levels across in the tunnelling gap, is present in all tunnelling systems, be they metallic, semiconducting or chemical. When IETS is performed between metal electrodes, the tunnelling junction is cooled to cryogenic temperatures to increase resolution. A biological system must work at ambient or body temperature, i.e. at ~300°K. Donor and acceptor levels across the tunnelling gap will therefore have a minimum width of 2 kT (~400 cm^{-1}). The range 0–4000 cm^{-1} could therefore be covered by 10 or so receptor types. A similar arrangement exists in the other spectral senses, vision and hearing, in which broadly tuned receptor classes cover segments of the complete spectrum.

Evidence for electron tunnelling in putative olfactory receptors

If olfactory receptor proteins function as a tunnelling spectroscope, their primary amino acid sequences may contain some telltale features, provided these are not too widely scattered and brought together only by folding. Firstly, since most odorants are redox-inactive, the receptor protein must obtain electrons from either a soluble electron carrier or possibly a reductase. If no intermediate enzyme is involved, one would expect to find a motif designed for binding to soluble electron donors. Secondly, the presence of a metal-binding site would not be unexpected, since many electron-transfer enzymes require metal cofactors. Thirdly, since the electron current must be turned into a chemical reaction at some point to connect it to the conventional signal transduction pathway, one would expect an electrochemical (e.g. a reduction) step to be the final stage in the transduction.

The sequences of 25 putative olfactory and eight

gustatory receptors have been published. They have strong homologies with G-protein-coupled receptors, are specific to olfactory neuroepithelia and contain a variable hydrophobic region which may be involved in odorant binding. The first step was to test for the presence of an NAD(P)H binding site motif in these sequences. The searches were performed using the Blitz server at Heidelberg. NAD(P)H binding motifs are highly conserved (Lawton *et al.*, 1990; Scrutton *et al.*, 1990). Remarkably, an exact match to an NAD(P)H binding site sequence (GLGLLA) highly conserved in dehydrogenases and flavine monooxygenases is found in one of the olfactory receptors, olf8_mouse, and related sequences are found in all the others. Since according to this theory the receptor functions as an 'NADPH diaphorase', it may be significant that high levels of diaphorase activity have been detected in olfactory receptor neurons (Zhao *et al.*, 1994).

The second step was to look for a metal-binding site. A clue as to which metal may be involved is provided by the evidence of a strong link between zinc and olfaction. Zinc deficiency, whether dietary (Alpers, 1994) or caused by treatment with histidine (Henkin *et al.*, 1975), thiocarbamides (Erikssen *et al.*, 1975) or captopril (Zumkley *et al.*, 1985), is unique in causing a complete and rapidly reversible anosmia. A search for zinc-binding sites found in enzymes using Prosite gave no good matches. A search for homologies was then performed using small segments of the primary sequence close to the flavin-binding site, the rationale being that the electron circuit is likely to be compact in size to avoid long-range transfer, and that this may be reflected in the primary structure. This search turned up a motif C[GATV]SH[LI], present in all the receptors, most commonly as CGSHL (Cys-Gly-Ser-His-Leu) seven amino acids away from the 'flavin-binding' region. This motif lies near the cytoplasmic end of the (predicted) sixth transmembrane domain and is absent from other G-protein-coupled receptors (Figure 2). CGSHL is the zinc-binding motif of insulins (Hodgkin, 1974). In insulin, several molecules coordinate around a single zinc ion via the histidine in the motif to form oligomers during storage in the pancreas. Perhaps surprisingly, this five-residue sequence is rare. In a search in the complete Swissprot database, 64 proteins gave an exact match to CGSHL. Ten of these were olfactory or gustatory receptors and 51 were insulins or proinsulins. Only three were neither olfactory receptors nor insulins: bombyxin B-8 precursor, alpha methyldopa hypersensitive protein and chitinase. These three extraneous proteins are unrelated to one another. Searches with the alternative sequences found in the olfactory receptors CASHL, CVSHL CTSHL and CSSHL give figures for unrelated/total of 5/11, 0/2, 0/6 and 8/10 respectively. With these few exceptions, therefore, the motif appears to be diagnostic of olfactory receptors and the zinc-binding site of insulins.

Zinc's involvement in olfaction, its ability to form bridges between proteins, its presence in electron transfer enzymes such as alcohol dehydrogenase (Fraùsto da Silva and Williams, 1993) and the presence of the redox-active amino acid cysteine in the receptor's zinc-binding motif all point to a possible link between electron flow and G-protein transduction. In the closely related adrenergic receptors, a role for cyclic reduction and oxidation of disulphide bridges has been suggested (Kuhl, 1985). It involves cross-linking of the G-protein to the receptor by an S–S bridge which is then reduced upon binding of the (redox-active) catecholamine to the receptor, thereby releasing the G-protein. I propose that a similar mechanism may be at work in olfaction (Figure 1). Suppose that the zinc-binding motif on the olfactory receptor is involved in docking to the olfactory G-protein g(olf), and that the docking involves formation of a disulphide bridge between the receptor and the g-protein. One would expect to find on g(olf) the other half of a zinc coordination site, e.g. two histidines in close proximity and a cysteine nearby. A search in the primary sequence of g(olf) (Jones and Reed, 1989) found the motif HYCYPH (His-Tyr-Cys-Tyr-Pro-His) at positions 343–351. This motif has the requisite properties for docking (Figure 3A): it is exposed on the surface of the g-protein (Coleman *et al.*, 1994; Lambright *et al.*, 1996) and is known to interact with g-protein-coupled receptors (Rasenick *et al.*, 1994).

The docking scheme was tested by molecular modelling of the two sequences. Figure 3 shows that when the three histidines coordinate a zinc ion, the minimum-energy configuration incorporating a disulphide bridge puts the two sulphurs very close to the zinc with no intervening group. The proline bend in the g(olf) motif helps bring the two histidines close together without strain. Reduction of the disulphide bridge followed by energy minimization causes little change in the structure, indicating that the redox reaction could take place reversibly at near-constant configuration energy. I have modelled every one of the zinc-binding motif variants in the proposed zinc binding configuration and found that the different side chains makes little difference to zinc binding and overall geometry. This

INS_RABIT	FVNQHL	CGSHL	VEALYLVCG
OLFO_RAT	GICKVFST	CGSHL	SVVSLFY GTIIGLYLCP
OLF1_CHICK	KDGKYKAFST	CTSHL	MAVSL FHGTVIFMYL
OLF1_RAT	VRGIHKIFST	CGSHL	SVVSL FYGTIIGLYL
OLF2_CHICK	KDGKYKAFST	CTSHL	MAVSL FHGTVIFMYL
OLF2_RAT	TVQGKYKAFST	CASHL	SIVS LFYSTGLGVY
OLF3_CHICK	KDGKYKAFST	CTSHL	MAVSL FHGTVIFMYL
OLF3_MOUSE	VEGRRKAFNT	CVSHL	VVVFL FYGSAIYGYL
OLF3_RAT	VHGKYKAFST	CASHL	SVVSL FYCTGLGVYL
OLF4_CHICK	KDGKYKAFST	CTSHL	MAVSL FHGTVIFMYL
OLF4_MOUSE	REGKFKAFST	CSTHI	SAVAI FYGSGAFTYL
OLF4_RAT	IQDIYKVFST	CGSHL	SVVTL FYGTIFGIYL
OLF5_CHICK	KDGKYKAFST	CTSHL	MAVSL FHGTVIFMYL
OLF5_MOUSE	ATGQRKAFST	CASHL	TVVVI FYTAVIFMYV
OLF5_RAT	PRGGWKSFST	CGSHL	AVVCL FYGTVIAVYF
OLF6_CHICK	KERKYKAFST	CTSHL	MAVSL FHGTIVFMYF
OLF6_RAT	IPSARGRHRAFST	CSSHL	TV VLIWYGSTIF
OLF7_MOUSE	EEGQRKAFST	CSSHL	CVVGL FYGTAIVMYV
OLF7_RAT	AAGRHKAFST	CASHL	TVVIIFYAAS
OLF8_MOUSE	KGWSKALGT	CGSHI	TVSLFYGSGLLAYVK
OLF8_RAT	SIHKVFST	CGSHL	SVVSLFY GTIIGLYLCP
OLF9_RAT	SIHKVFST	CGSHL	SVVSLFY GTIIGLYLCP
OLFD_CANFA	IGICKVFST	CGSHL	SVVSLF YGTVIGLYLC
OLFE_HUMAN	VSKKYKAFST	CASHL	GAVSL FYGTLCMVYL
OLFI_HUMAN	SKGICKAFST	CGSHL	SVVSL FYGTVIGLYL
OLFJ_HUMAN	VEGRKKAFAT	CASHL	TVVIV HYSCASIAYL
GU58_RAT	SQGKYKAFST	CASHL	SVVSLFYSTLLGVYL
GU33_RAT	SSTVSKYKAFST	CGSHL	CVVCLFYGSVIGV
GU38_RAT	SLLGGMYKAFST	CGSHL	SVVSLFYGTGFGV
GU45_RAT	SSAEGKYKAFST	CVSHL	SVVSLFYCTLLGV

Figure 2 Sequence homologies between insulin (top line) and olfactory and gustatory receptors. The motif indicated in red (box) is the zinc-binding motif of insulin, which is also present in all the olfactory and gustatory receptors with small variations. The blue motif of olf8_mouse is a highly conserved NADPH binding sequence.

zinc–thiol site may be the electron outlet, the positive connector of the olfactory transducer.

The odorant-binding site may lie somewhere in between the flavin and the zinc-binding motifs. Note that its intracellular location poses no problems of accessibility to odorants: they are small hydrophobic molecules which will typically partition into membranes with partition coefficients of the order of 10^3. These findings suggest that future attempts to express or reconstitute receptors should include zinc and an electron donor in the cytoplasmic phase before testing for response to odorants. It is not clear as yet whether the corresponding sequences in other receptors are capable of binding electron acceptors. It may be that a range of acceptor sites capable of binding donors at different redox potentials is required to probe different segments of the spectrum, and that no single sequence can serve for all.

Neurophysiological evidence

There is evidence that single olfactory receptor neurons (ORNs) can respond to several odorants (Sicard and Holley, 1984). This is consistent with the idea that they respond to a feature common to several molecules. Is the feature structural or vibrational? If the latter, one would expect the responses of ORNs to different odorants to correlate with

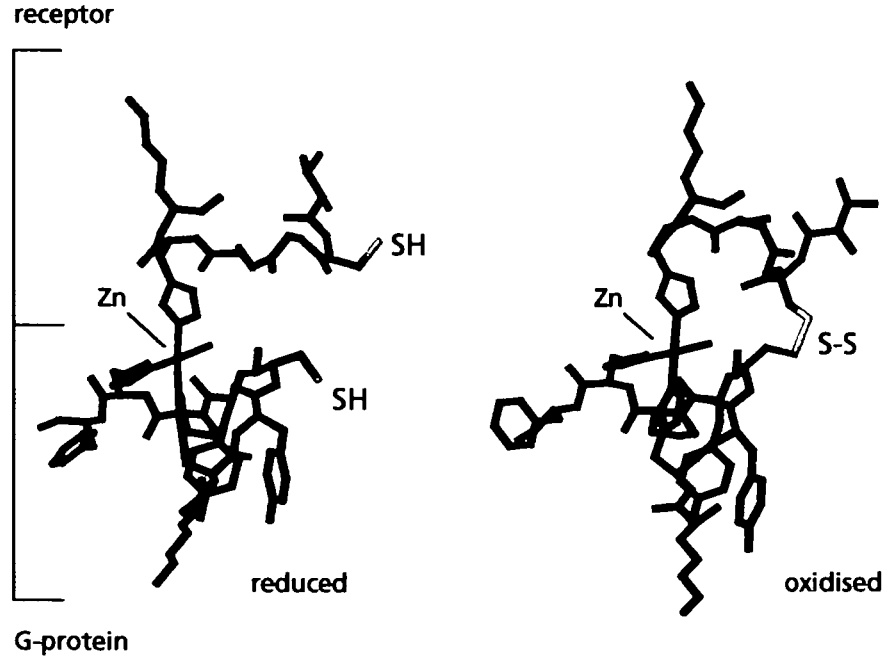

Figure 3 Proposed docking scheme between the receptor protein (top half of structures) and the G-protein (bottom half). The structures were obtained using MM2 Mechanics (Cache). The TCGSHL (receptor) and HYCYPH (G-protein) sequences were aligned, coordination bonds to zinc (purple) were made from three histidines, the S–S bond was connected and the structure was allowed to relax to minimum energy (right). The S–S bond was then broken and reduced, and the structure was allowed to relax again to minimum energy. Little movement of the overall structure occurred apart from separation of the SH groups, suggesting that the process can be reversed.

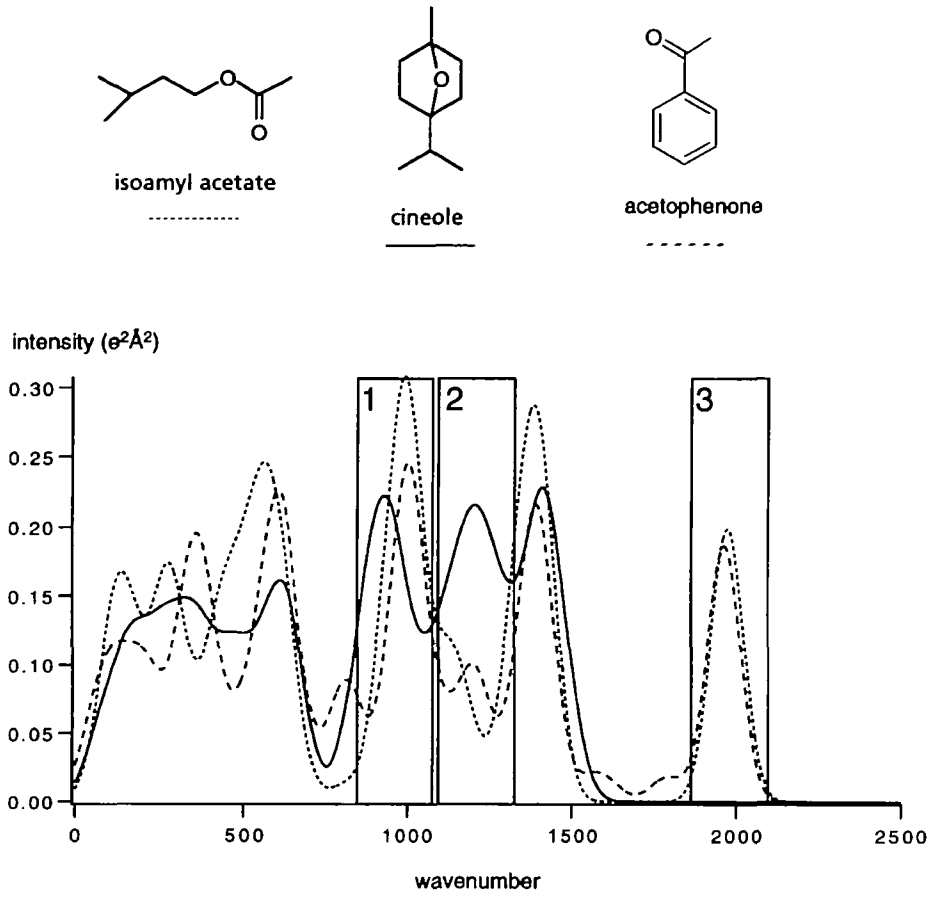

Figure 4 Structures (top) and CHYPRE spectra (bottom) of three odorants used by Firestein *et al.* (1993) in experiments in which the responses of single olfactory receptor neurons were measured. Figure 1 of their article illustrates a cell responding only to isoamyl acetate and acetophenone, one cell responding to all three and one cell responding to cineole but not to the other two. This pattern of responses is consistent with the cells being tuned respectively to bands 3, 1 and 2 of the vibrational spectrum (see text).

vibrational spectra. Furthermore, ORNs are known to express only one or a small number of receptor genes (Ressler *et al.*, 1994). Their response patterns should therefore be consistent with each ORN responding to one, or possibly a few, vibrational bands. It has recently become possible to record from isolated olfactory receptor neurons using patch-clamp methods. The most direct evidence (Firestein *et al.*, 1993) for comes from a study of isolated salamander olfactory neurons exposed to three odorants: cineole, isoamyl acetate and acetophenone. Cells were found that responded in all the possible patterns to one odorant, two odorants or all three. The response pattern of three cells, taken from figure 1 of Firestein *et al.*'s paper, is as follows: one cell responded to all three odorants, one cell to acetophenone and isoamyl acetate but not to cineole, and one to cineole alone. When the spectra of the three odorants are calculated using an algorithm which simulates tunnelling spectra (see below), the results of Firestein *et al.* are consistent with their sensing three different vibrational bands (Figure 4). The cell responding only to cineole could have been tuned to the band at ~1200 cm^{-1} which is largely absent in the other two odorants. The cell responding to all three may have been sensitive to the band at ~1000 cm^{-1}, and the cell responding only to acetophenone and isoamyl acetate may have been responding to the C=O stretch at ~1800. By contrast, it is far from clear which structural features would account for this pattern. The vibrational theory could readily be tested by further experiments: the cells responding to the C=O stretch should respond to a nitrile, while the cell responding only to acetophenone should also respond to benzene and possibly to an alkene.

Calculating odours: a first approximation

The proper test of a structure–odour theory is odour prediction. If electron tunnelling is the means by which molecules are recognized, then their tunnelling spectra as

measured by the biological detector should correlate with their odour. Spectral comparison requires three independent pieces of information: the frequency of a given vibrational mode, its intensity as perceived by the sensor and the resolution of the detector system. The first is reasonably easy to obtain: semi-empirical quantum chemistry programs calculate most vibrational mode frequencies to an accuracy of the order of 50 cm^{-1}, i.e. much greater than the assumed sensor resolution. As was discussed before, a resolution of the order of ~400 cm^{-1} is the best that can be expected. Line intensities are more of a problem: if, for example, Raman spectra of dyes with absorption lines in the visible were compared with perceived colour, no correlation would be found. This is because the pigments in the photoreceptors operate by a mechanism involving absorption, not Raman scattering. Furthermore, prediction of the perceived colour of a dye from its absorption spectrum requires knowledge of the number of pigments present in the retina and their spectral resolution.

IETS spectra of different compounds in metal–insulator–metal junctions have been measured, and a theory for calculating their line intensities has been developed. Unfortunately odorants are not well-suited to conventional IETS measurements, because they tend to evaporate during the vacuum deposition steps used in the manufacture of the tunnelling junctions. From a theoretical standpoint, another problem exists. Line intensities in conventional IETS are determined in part by the image charges caused by the close proximity of metal surfaces with their effectively infinite dielectric constant. In a biological sensor, dielectric constants will vary over a much smaller range, bounded by 3–5 for protein and 80 for water. Therefore, even if measured IETS spectra of odorants were available, they would not necessarily correlate well with those detected by a biological sensor.

I have developed an algorithm for the calculation of 'biological' IETS spectra called CHYPRE (for CHaracter PREdiction). Three steps are involved: the first is calculation of the $6N - 6$ (where N is the number of atoms) vibrational mode frequencies and $N(6N - 6)$ atom displacements, using MOPAC with PM3 parameters. This will be most reliable when calculating molecules which do not contain nitrogen, which fortunately is the case for most odorants. The second step involves calculation of partial charges. This is important because electron scattering is proportional not to overall dipole moments but to the square of the partial charge. Partial charges are not direct observables, and therefore the choice of algorithm and parameters for their calculation is to some extent arbitrary. In all the calculations shown below Zindo with INDO/1 parameters was used because it gives the best correlation between the computed spectrum and smell (see below). Both MOPAC and Zindo form part of the CaCHE Worksystem (Oxford Molecular) which was used in all the calculations.

The core of the CHYPRE algorithm calculates a 'biological IETS' spectrum according to the theory developed by Sleigh *et al.* (1986), modified to take into account the fact that rotation of the molecule is likely to occur because of the weakness of the forces (hydrogen bonds and dispersion forces) binding it to the receptor, and neglecting image charges. Details of the algorithm will be published at a later date. For the purpose of the present article, it should be emphasized that all molecules were calculated using identical parameters and that, unless otherwise indicated, no scaling of the spectra was involved. To mimic the thermal broadening of lines in a biological system, spectra were convolved with a Gaussian blurring function with a standard deviation of 200 cm^{-1}. The most obvious difference between computed IR and CHYPRE spectra is that the fingerprint region below 1500 cm^{-1}, used by spectroscopists to determine molecular structure, is emphasized more by CHYPRE than by IR. This fits empirical odour data, because most of the differences between odorants with similar elemental composition and different structures will be concentrated in this region.

Two examples of vibrational structure–odour relations

A good test of the CHYPRE algorithm would be comparison of the spectra of two or more molecules with very similar odours and very different structures. Such an occurrence is rare, but enquiries among perfumers elicited one example, that of the chemically unrelated ambergris odorants cedramber, karanal, Jeger's ketal and timberol (Figure 5). The ambergris note of the four is very similar, karanal being slightly greener than Jeger's ketal, with cedramber and timberol somewhat woodier. The upper graph in Figure 5 illustrates the raw (unconvolved) data from CHYPRE calculations. Each point on the graph represents a vibrational mode, with wave number along the abscissa and intensity along the ordinate. A considerable amount of scatter is present, showing that these three

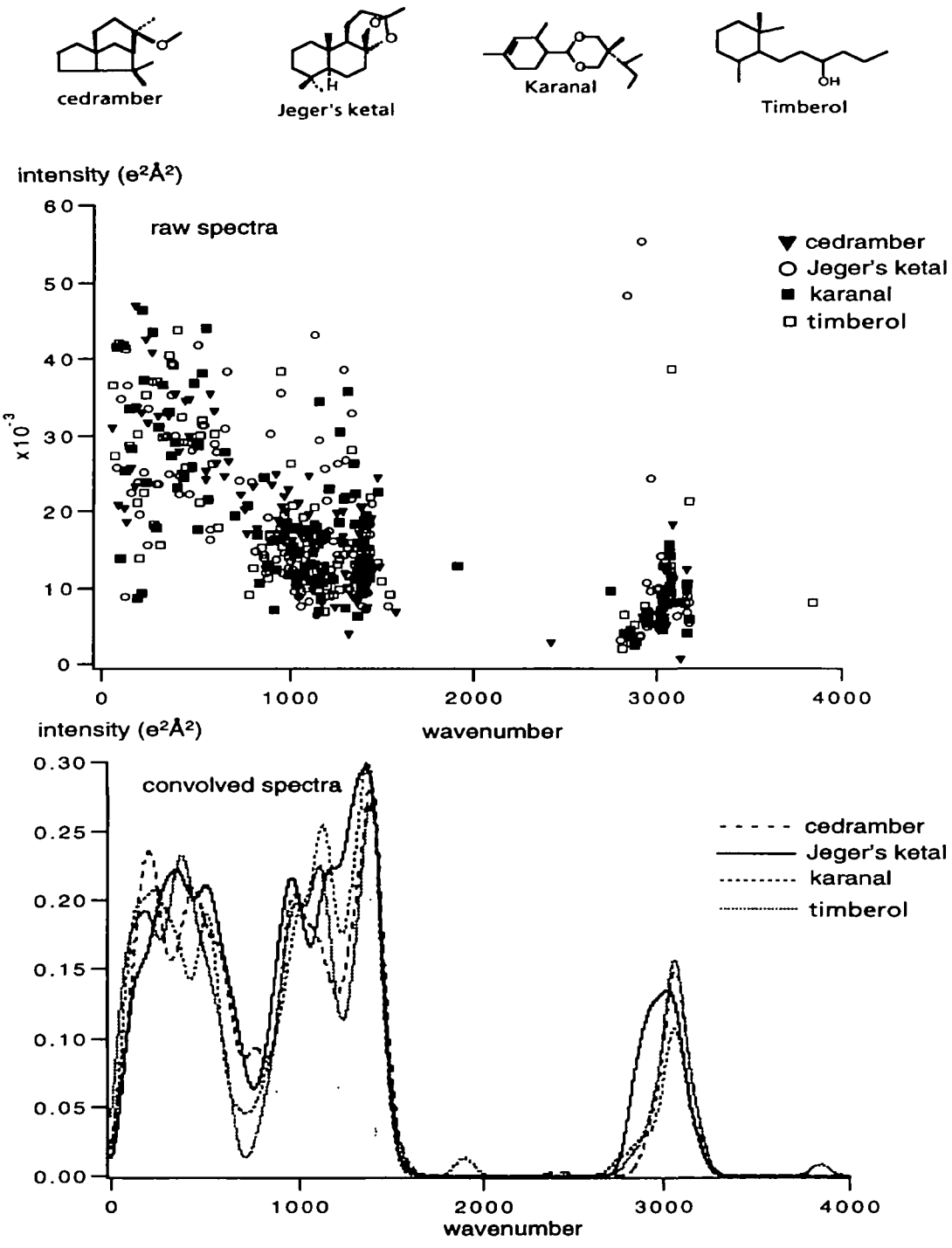

Figure 5 Structures (top), raw vibrational spectra from CHYPRE calculations (middle) and convolved spectra (bottom) for four ambergris odorants with closely related odours and very different structures. Each point in the raw spectra represents the energy and amplitude of a single vibrational mode. A considerable degree of scatter is present, reflecting the structural diversity of the molecules. By contrast, the convolved CHYPRE spectra, like the odours, are remarkably similar.

chemically unrelated molecules have very different underlying vibrational modes and partial charges. After convolution, however (lower graph), the spectra become very similar, consistent with their similar smells. The relationship between structure and odour is thus subject to two encoding steps: from structure to vibrational modes, and from vibrational modes to perceived convolved spectrum.

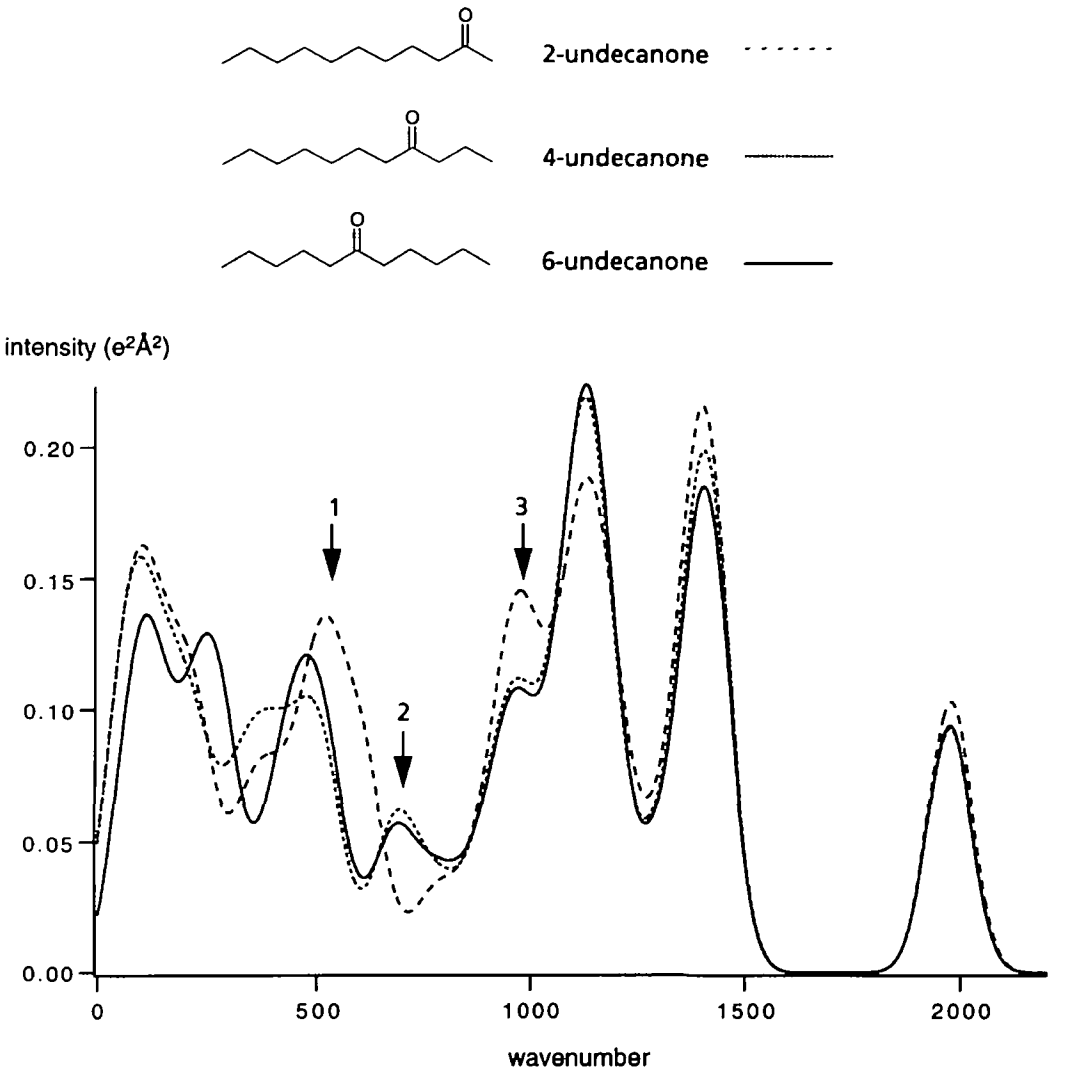

Figure 6 Structures (top) and CHYPRE spectra (bottom) of three undecanones differing in the position of the carbonyl group. Moving the carbonyl from position 4 to position 6 markedly affects the position and intensities of three convolved peaks indicated by the arrows. Like their odour character, the spectrum of 4-undecanone is intermediate between that of the 2 and 6- isomers, except in the 5–600 cm^{-1} region, where it follows closely that.of 2-undecanone.

The converse experiment should also be true, namely that molecules with very similar structures and different smells should have different spectra. Figure 6 illustrates the CHYPRE spectra of the well-know example (Ohloff, 1986) of three undecanones differing in the position of the carbonyl group. 2-Undecanone smells of ruewort, 6-undecanone smells fruity and 4-undecanone is reportedly intermediate in odour between the two. Despite the close structural similarity, the spectra of 2- and 6-undecanone are clearly different. Peak 1 differs in amplitude and is shifted by 100 cm^{-1}, and peaks 2 and 3 differ in amplitude. This suggests that the ability of the olfactory system to discriminate closely related molecules could be achieved by a vibrational transduction mechanism.

Six ways of being odourless

A peculiar feature of a vibrational theory is that since all molecules vibrate, they should all have an odour (provided of course they are volatile) unless some other factors peculiar to the function of a biological spectroscope prevent electron tunnelling from taking place.

No partial charges

A typical example of this are the homonuclear diatomic gases such as H_2, N_2 and O_2. Molecules made up of two identical atoms can have no partial charges on their atoms for reasons of symmetry and would be predicted to be odourless, which they are. The apparent exception of

halogen gases, e.g. Cl_2, cannot be settled at present, because they cause an intense trigeminal sensation of pungency and immediately react with biological molecules to form chloramines, which themselves have an intense 'chlorine' smell.

Too big

Odorants are all <400 daltons or so in molecular weight. Larger molecules, while they may develop appreciable partial pressures, are odourless. Near the maximum size, many specific anosmias are known to exist. For example, most subjects are anosmic to one or another of the large musks such as pentadecanolide or Tonalide. According to this theory, if a small change to a large molecule renders it completely odourless, as opposed to less odorant or nondescript in character, it is likely to be because it no longer fits any receptor. Note that a maximum size follows naturally from a tunnelling theory. All other things being equal, tunnelling probabilities across a gap of length d are proportional to $\exp(-d^2)$, so that the size requirement may reflect the inability of a tunnelling sensor to give appreciable currents over distances >1–2 nm.

Blind spots

The tunnelling gap must contain something, either water molecules or more probably side chains of hydrophobic amino acids. If the latter is the case, then receptors tuned to the broad C–H stretch frequency would be fully switched on all the time, which would probably cause rapid habituation. A more likely possibility, since C–H stretch will be too common in any event to distinguish molecules from one another, is that such a band is simply not represented in the spectrum, and that one or more receptor bands are missing. This would account, for example, for the fact that CH_4 is odourless, though weak scattering (see below) may also contribute. A second type of blind spot might arise if a band is never represented in odorants, thus making the receptor class redundant. One example might be the 2600–2800 band between SH stretch and the lowest aldehyde CH stretches.

Frequencies too low

Vibrational modes below kT will not be detected by a biological spectroscope for two reasons: firstly, they will already be thermally excited, and electrons will be as likely to gain energy from them as to excite them to a higher vibrational level. This will reduce the tunnelling current.

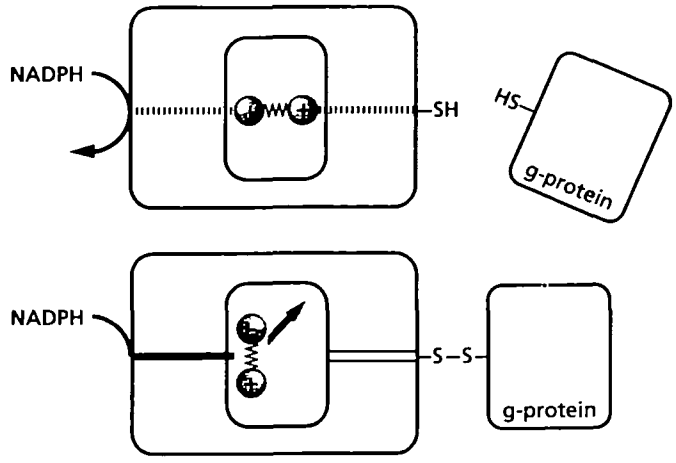

Figure 7 Influence of scattering group orientation on electron tunnelling. Scattering from a dipolar group with a clearly defined direction of charge movement will cause the electrons to change direction as well as energy. If the dipole movement is parallel to the tunnelling path (top) the electrons will continue in a straight line. If the dipole oscillates at right angles to the tunnelling path, electrons will be scattered sideways. In this schematic the donor and acceptor sites are arranged in such a way that electrons scattered transversely do not reach the acceptor site, and therefore cannot reduce the disulphide bridge to effect G-protein transduction

Secondly, if the difference in energy between donor and acceptor levels is of the order of kT, thermal broadening of the levels will mean that electrons will flow whether or not an odorant is present, and the problem reduces to that of the blind spot discussed above. The tetrahalomethanes CCl_4, CBr_4 and CI_4 provide a test of this idea. The first two have (different) distinctive haloalkane odours, but CI_4 is odourless and merely smells weakly of its decomposition product, iodine. CCl_4 (459 and 790 cm^{-1}) and CBr_4 (267 and 671 cm^{-1}) have modes above kT, but all the modes of CI_4 (90, 123 and 178 cm^{-1}) except one lie below kT (Dollish *et al.*, 1974). This is consistent with the lower limit of frequencies being between kT and 2kT.

Scattering too weak

Taking the simplest case of a diatomic molecule as an example, scattering will be proportional to the square of atom displacements. Stiff bonds carrying small partial charges will have low line intensities. For example, CHYPRE calculates very low line intensities for the C=C stretch (see the discussion of bitter almonds below) and a low intensity for the stretch band in carbon monoxide, which may explain why it is odourless despite being a heteronuclear diatomic and a potential odorant.

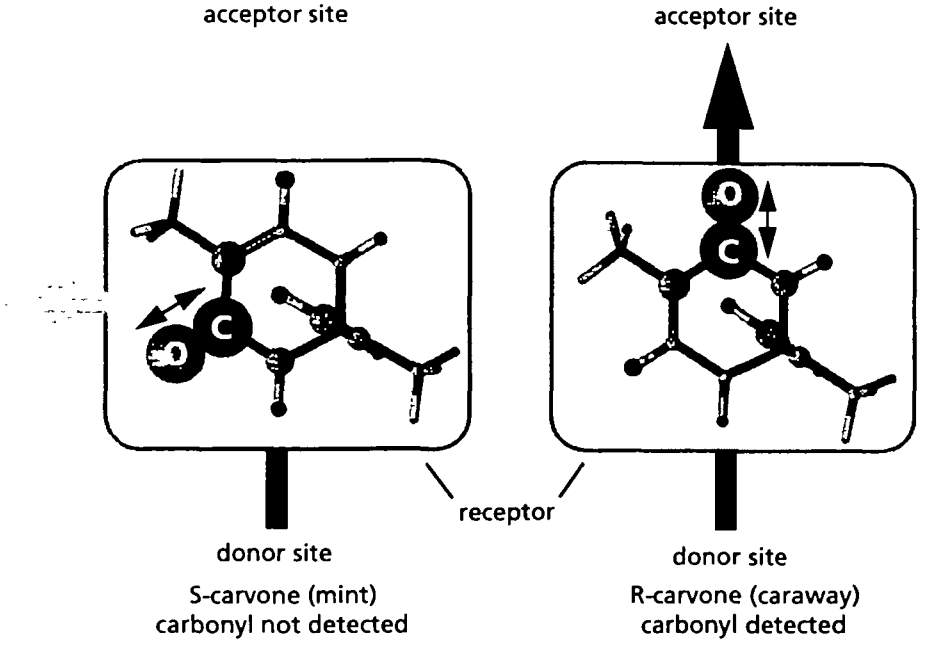

Figure 8 Application of the geometric principle illustrated in Figure 7 to the problem of carvone enantiomers The two carvones are shown here as ball and stick models, with the diameter of the balls proportional to the partial charge on the atom (Mopac, PM3 parameters). The C=O bond carries by far the largest dipole in the molecule. The isopropenyl moiety (bottom right of the molecule) is shown pointing towards the reader in the same orientation in both enantiomers, consistent with the fact that energy barriers to rotation of the isopropenyl group are very low If the carvones fit into the receptor in the same overall orientation, the two carbonyl groups will be oriented at 120° to one another. If, in R-carvone (right), the carbonyl is correctly aligned with respect to the electron path and is therefore detected, then in S-carvone (left) the carbonyl will be nearly at right angles to the electron path and will scatter the electrons in such a way that they do not reach the acceptor site. The rest of the molecule is perceived identically in both, because no other prominent dipoles are present. The prediction is therefore that adding back the C=O vibrations (carried by, say, butanone) to the smell of S-carvone should turn its odour character from mint to caraway, which it does.

Wrong relative group orientation

An unusual feature of a protein-based spectroscope is that it exhibits polarization effects. When scattered, electrons change direction as well as momentum. For example, they will be scattered sideways if the scattering vibration takes place at right angles to the tunnelling path (Figure 7). In conventional IETS, this lengthens their path across the insulating gap and reduces their tunnelling probability. In a biological sensor, where donor and acceptor sites on either side of the tunnelling gap are likely to have a small cross-section, electrons scattered in the wrong direction may fail to reach the acceptor site altogether, and the sensor will not respond. The effect will be clearest when the vibration involves only two atoms, with a well-defined direction of charge movement. This will ensure that electrons are scattered in a preferred direction. The scattering group must be fixed with respect to the rest of the molecule, which must in turn assume a preferred orientation with respect to the sensor. Flat rings bearing intense scatterers as substituents are ideal in this respect. What will happen in this case is that only *part* of the molecule will be odorant, and that the smell character will resemble that of the molecule with the 'hidden' (transverse scattering) group removed. Examples of this effect are discussed in the next section.

'Hidden' dipolar groups

The puzzle of carvone enantiomers

A persistent objection to the infrared-spectrum theory has been that, unlike our nose, it could not resolve enantiomers. While it is true that solution spectra of enantiomers are identical, the objection does not apply to a protein-based sensor. One reason, common to all receptors, is that odorant-binding sites in the sensors are always chiral to some extent, and their relative affinities for enantiomers therefore differ. Interestingly, discrimination between carvone enantiomers in a neurophysiological preparation has been shown to fall with rising temperature (Hanada *et al.*, 1994), consistent with the idea that weak (e.g. Van der Waals) forces hold the odorant in a particular orientation in the receptor.

Another reason, discussed above, is that part of the

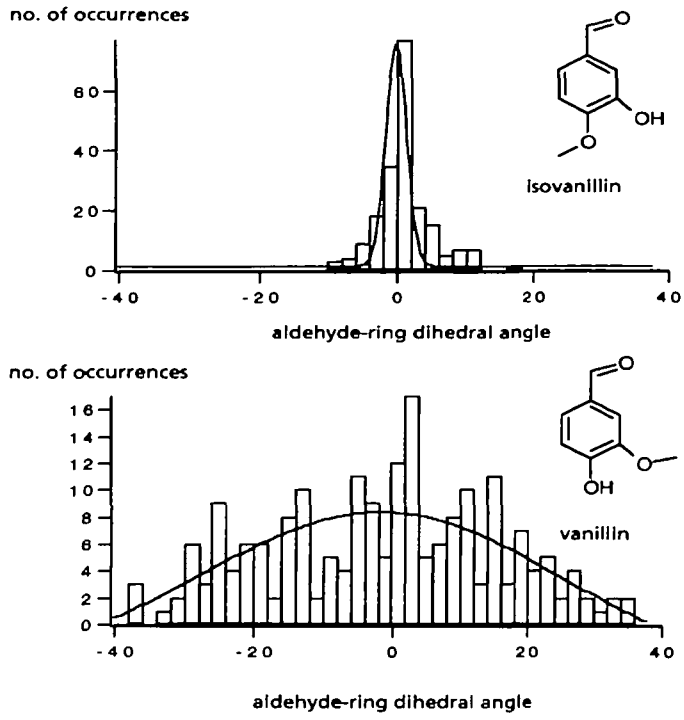

Figure 9 An example of the influence of a dynamic effect of group orientation on odour character. Optimal structures and partial charges were calculated using Mopac with AM1 partial charges, and the molecular dynamics were run using MM2 dynamics. Temperature, 300 K; equilibration time, 1 ps; dynamics run, 4ps; measurement every 20 fs. The histograms show the dihedral angle between the aldehyde group and the phenyl ring during the simulations. The curves are Gaussian fits. In isovanillin (top) the aldehyde group is held rigidly parallel to the ring (SD 20°), while in vanillin the aldehyde rotates more freely (SD 37°). I propose that, as in carvones, theorientation of the aldehyde group in isovanillin is such that it is not detected, and that isovanillin should therefore smell of guaiacol, which it does.

molecule may be 'invisible' to the receptor because of the unfavourable orientation of a dipolar group. This idea can be applied to the odorant couple S(+) and R(–) carvone. The two isomers smell respectively of mint and caraway (Arctander, 1994). Inspection of their calculated optimal configuration shows that if the cyclohexene ring and its projecting (and freely rotating) isopropenyl substituent bind to the receptor in fixed orientation with respect to the main axis of the molecule, the two carbonyl groups lie at 120° to one another (Figure 8). The carbonyls also bear the largest partial charges, so they should dominate electron scattering and the odour character. If (+) and (–) carvone smell different because the carbonyl in one of the two isomers is detected less intensely, replacement of that carbonyl group should be without much effect on odour. Since many other mint odorants do not contain a carbonyl, one suspects that S-carvone is the isomer in which the C=O group is silent. This prediction is borne out by experiment: (–) carvol, where the C=O is replaced by C–OH, retains the minty odour (Weyerstahl, 1994). By contrast, the same replacement in (+) carvone alters the odour character completely.

If this theory is correct, 'adding back' some carbonyl vibrations to R(–)-carvone should shift its odour character from mint to caraway. This can be done by mixing R(–)-carvone with a molecule with a simple vibrational spectrum dominated by a C=O stretch, e.g. 2-pentanone. Indeed, a 3:2 v/v mixture of 2-pentanone and R(–)-carvone loses much of its mint character and acquires a definite caraway note.

Aldehyde rotation in vanillin isomers

The different odours of vanillin and isovanillin are a classic olfactory conundrum. The two molecules differ only in the position of their substituents on the benzene group. Vanillin has a rich vanilla odour whereas isovanillin has a weaker, very different, somewhat phenolic odour. As may be expected from their close similarity of structure, the vibrational spectra of vanillin and isovanillin are very similar. Molecular dynamics simulations of the two molecules, however, reveal an essential difference (Figure 9). In isovanillin the aldehyde group is constrained to lie in the plane of the benzene ring. In vanillin, by contrast, rotation about the bond joining the aldehyde to the benzene ring is easier, and the aldehyde can adopt a range of configurations more nearly orthogonal to the ring. I suggest that it is this rotation that makes detection of the carbonyl possible in vanillin. In isovanillin the carbonyl group is transversely oriented and therefore undetectable. One would therefore expect isovanillin to smell like its aldehyde-less congener guaiacol, i.e. phenolic–medicinal. This is the case: perceptually, isovanillin, though not entirely devoid of vanilla character (Arctander, 1994), possibly reflecting infrequent aldehyde rotations, is closer to guaiacol.

As in the case of carvones, an 'additive synthesis' of the vanillin smell is possible by mixing guaiacol (phenolic) and ethylbenzaldehyde (bitter almonds). In the proximity of the 1:1 proportion, a vanillin-like note appears. The illusion is not perfect, but it is striking because the vanilla character is absent from the components. The CHYPRE spectra of benzaldehyde and guaiacol are shown in Figure 10, together with their sum (without scaling) and the spectrum of vanillin. The sum spectrum gives a reasonably good fit to the vanillin spectrum, consistent with the smell character of the mixture.

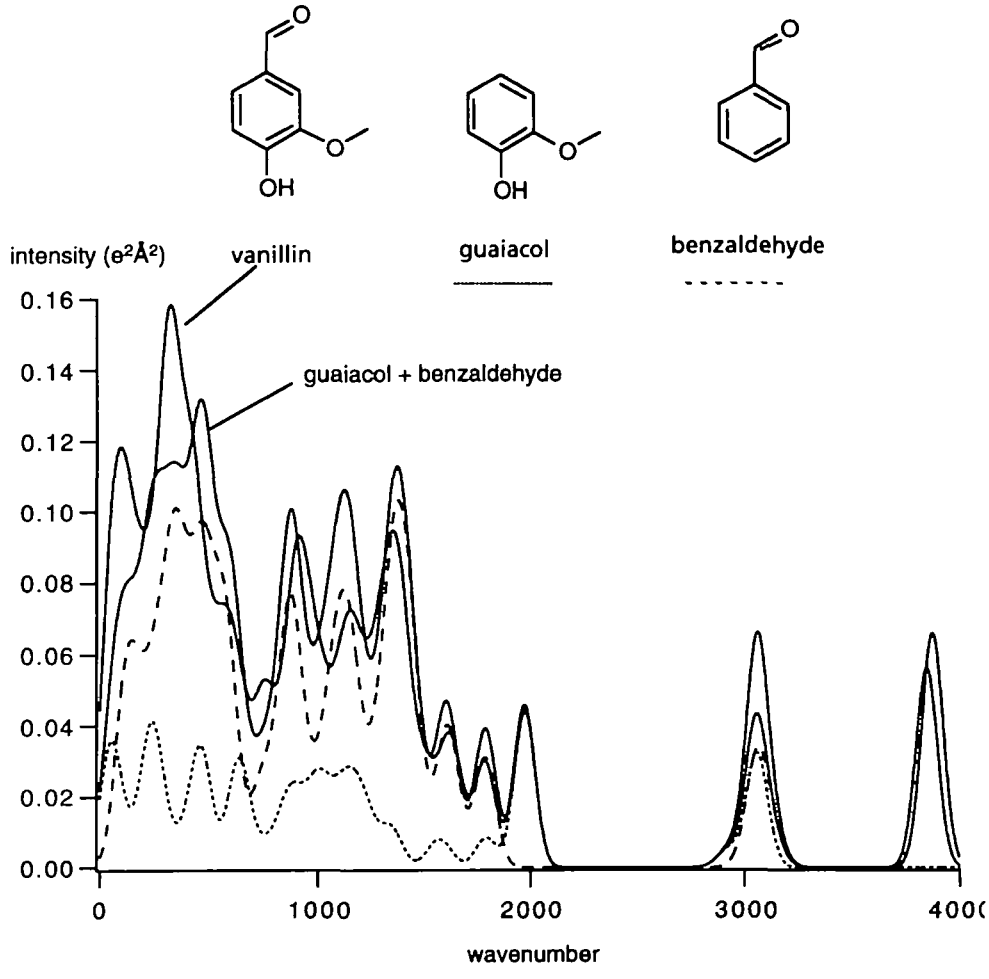

Figure 10 'Additive' synthesis of the odour of vanillin from vibrational components. The structures of vanillin, benzaldehyde and guaiacol are shown at the top, and the unscaled CHYPRE spectra for the three molecules at bottom. The sum of the spectra of guaiacol (phenolic, medicinal odour) and benzaldehyde (bitter almonds) gives a reasonable approximation to the spectrum of vanillin. A mixture of guaiacol and benzaldehyde is therefore predicted to have a vanilla odour character, which it does

Monochromatic odours: the 2500 and 2300 cm^{-1} bands

A simple test of a vibrational theory of olfaction would be a 'monochromatic' stimulus, i.e. a stimulus consisting of one frequency only. The region below 1500 cm^{-1} is unsuited to this approach, because organic molecules have most of their modes in this range and no obvious correlations between the mere presence of a vibration and an odour character exist. By contrast, the region between 1500 and 4000 cm^{-1} contains the stretch frequencies of various specific groups, and there appears to be a good correlation between some vibrational frequencies and odour character.

The most striking example is the 2500 cm^{-1} band. Mercaptans, selenomercaptans and telluromercaptans (R-SH, SeH and TeH) have a unique odour character, found in no other organic molecule. Their stretch vibration frequency (~2550 cm^{-1}) is equally unique, and does not overlap with any other common group frequency (Socrates, 1994). Remarkably, terminal boron–hydrogen (BH) group stretch frequencies at ~2600 are the only ones known to overlap S, Se and Te–H stretches (Nakamoto, 1986). Even more remarkably, the stable and relatively non-volatile borane $B_{10}H_{14}$ (decaborane; Sigma) is to my knowledge the only non-sulphur containing molecule that smells like a mercaptan. Other boranes reportedly smell similar. The next nearest (≤2400 cm^{-1}) are the P–H and As–H stretches of phosphine, arsine and their derivatives (Nakamoto, 1986). They reportedly smell of garlic and rotten cabbage (Klopping, 1971)—two sources of complex mercaptans—suggesting that their vibrational frequencies are close enough to excite a putative 2500 cm^{-1} receptor band. The existence of a congenital specific anosmia to mercaptans

(Amoore, 1971) is also consistent with a vibrational mechanism. If shape determines odour, it is difficult to understand how a mutation would wipe out a large number of receptors while only affecting a single odour class. By contrast, the absence of a receptor responsible for a unique frequency band will abolish detection, much as the absence of long-wavelength cones gives rise to protanopia. Other congenital anosmias, such as that to amines (Amoore, 1971) (~3300 cm^{-1}), may have a similar origin, and it will be interesting to re-examine them with molecules designed to probe different vibrational bands.

There may another band of interest just below the SH stretch band, at ~2300 cm^{-1}. Alkyl isothiocyanates (R–N=C=S, stretch frequency ~2200) have a unique mustard odour character, and so does the chemically unrelated carbon suboxide O=C=C=C=O (C=O stretch frequency ~2200). Another instance of a straightforward correlation between spectrum and smell is the aldehyde–nitrile replacement rule. It is well known to fragrance chemists that the nitrile group can frequently replace an aldehyde with only a minor change of odour character, 'duller' and somewhat 'oily' (Bedoukian, 1986). For example, benzaldehyde and benzonitrile have similar odours, as do agrunitril and citronellal, cinnamaldehyde and cinnamalva. This is consistent with vibrational detection, since the intense nitrile vibration at 2100 could replace the carbonyl band at ~1800 (Socrates, 1994). A receptor band 2kT wide centred at ~1900 cm^{-1} would cover both easily.

A 'bichromatic' odour : bitter almonds

The bitter almond character is shared by a large number of quite different small molecules with related but not identical odours. A recent study of quantitative structure–activity relationships of 40 bitter almond odorants concludes that the essential features are: small size, one or more C=C bonds and a 'hydrogen-bonding acceptor' group, namely aldehyde, nitrile or (with a more marked change in smell character) nitro (Zakarya *et al.*, 1993). Remarkably, the bitter almonds character is also shared by HCN, which, being a triatomic molecule, has only three vibrational modes, at 712 (bending mode), 2094 (CN stretch) and 3213 cm^{-1} (C-H stretch), and, of course, no double bonds. Can this be made sense of vibrationally?

The CN stretch of HCN, as we have seen earlier, is a good replacement for aldehydes and nitro groups. The requirement for a double bond is best illustrated by comparing the CHYPRE spectra of hexanal and *trans*-2-hexenal. Hexanal has a powerful, fatty green odour, whereas *trans*-2-hexenal (to most subjects) has a definite bitter almonds note in addition to a green character. The spectra differ chiefly in the amplitude of the two peaks at 1100 and 1400 cm^{-1}. One possibility is that the first harmonic of the v2 fundamental ($2v2 = 1412\ cm^{-1}$) (Choi and Barker, 1932), which gives an intense IR line, excites the 1400 band. This somewhat *ad hoc* idea cannot be excluded, but seems hard to reconcile with the fact that CHYPRE calculates rather low intensities for the 1500–1600 cm^{-1} C=C band (stiff bond, small partial charges). Another possibility is that the bending mode of HCN excites a receptor band lying between 700 and 1000 cm^{-1}. This would be consistent with the fact that the CHYPRE spectrum of cyclohexenal, which does not smell of bitter almonds (and therefore constitutes another exception to the 'structure–odour' rule), has no such peak. It also fits in with the spectra of other odorants with typical bitter almond odours, such as benzonitrile and benzaldehyde, all of which have intense bands at ~1000 cm^{-1}.

A counterintuitive structure–odour relationship: the aliphatic aldehydes

One of the most perplexing structure–odour relationships is that of aliphatic aldehydes. It is well known to perfumers that aldehydes between C-8 and C-12 fall into two groups according to the number of carbon atoms. Though each aldehyde smells different, even numbered ones tend to have fruity, orange-like odours, while odd numbered ones have a more floral (also described as waxy) character (Arctander, 1994). No such pattern is discernible in the corresponding alkanes or alkanols, suggesting that the aldehyde group is responsible. Remarkably, MM2 molecular dynamics reveals a systematic difference in rotational mobility of the aldehyde group around the C–C bond joining it to the rest of the molecule in the two groups (Figure 11a). In heptanal, nonanal and undecanal, the aldehyde rotates only by ~90° on either side of its lowest energy configuration. By contrast, in octanal, decanal and dodecanal it is free to rotate by a full 360°.

This is unlikely to be due to an artefact of MM2 molecular dynamics, because Mopac calculations show that the aldehydes fall into two distinct even and odd groups even when their vibrational properties are calculated from quantum rather than classical methods. Figure 11b shows

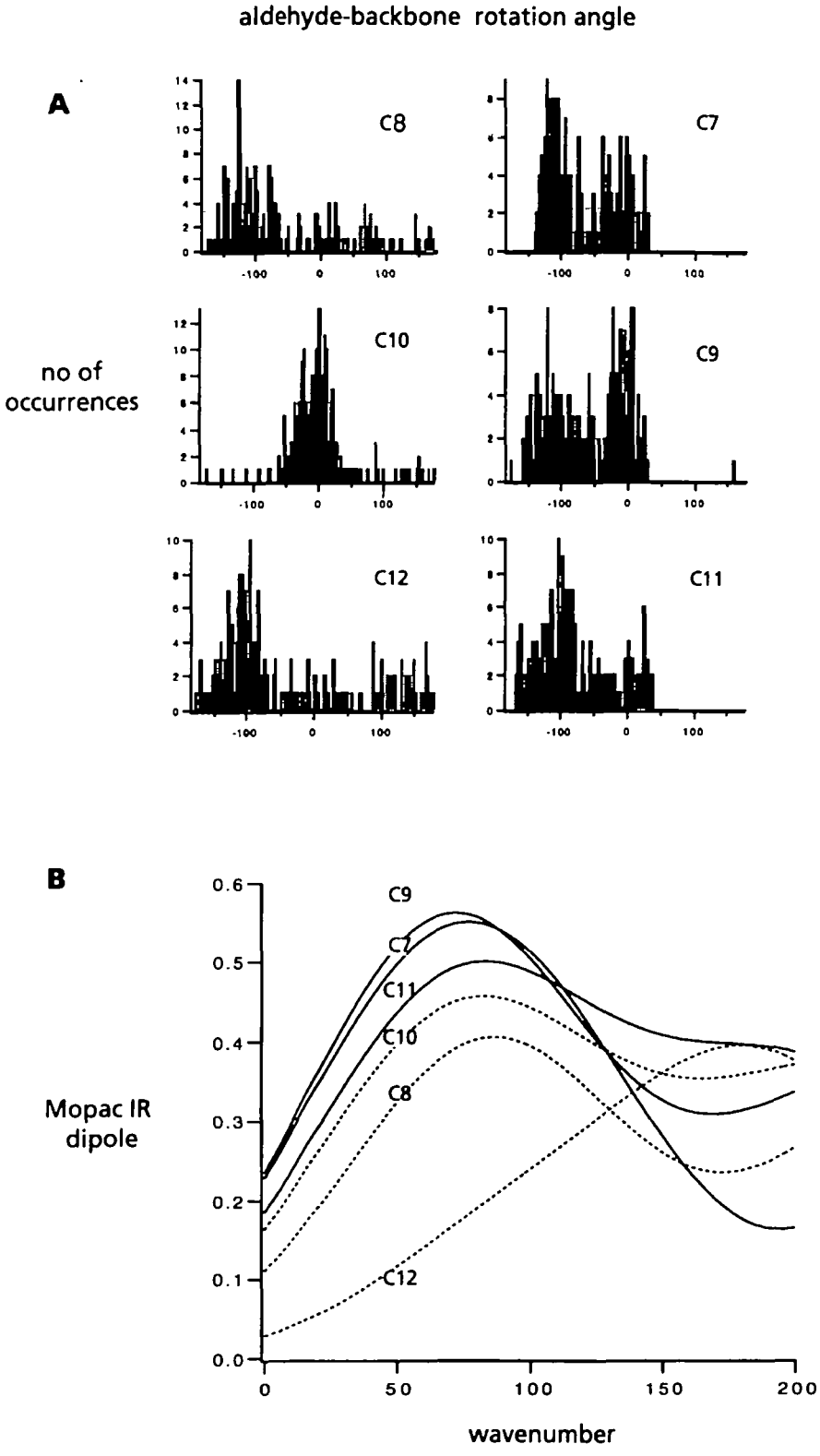

Figure 11 Rotational mobility of the aldehyde group in straight-chained aliphatic aldehydes. The histograms depict the distribution dihedral angle between the aldehyde group and the nearest CH_2 during a simulation run. Optimal structures and partial charges were calculated using Mopac with AM1 partial charges, and the molecular dynamics were run using MM2 dynamics. Temperature, 300 K; equilibration time, 1 ps; dynamics run, 4 ps; measurement every 20 fs. In the even-numbered aldehydes (left half) the aldehyde is more free to rotate and reaches portions of the phase space (grey histogram bars) which are not accessible to odd-numbered aldehydes (right half). This effect is not likely to be an artefact of the MM2 molecular dynamics. The modes which contribute to aldehyde rotation are low-energy twisting modes involving the whole molecules. The lower graph illustrates the calculated Mopac dipole strength for these modes. Even and odd aldehydes fall into two distinct groups.

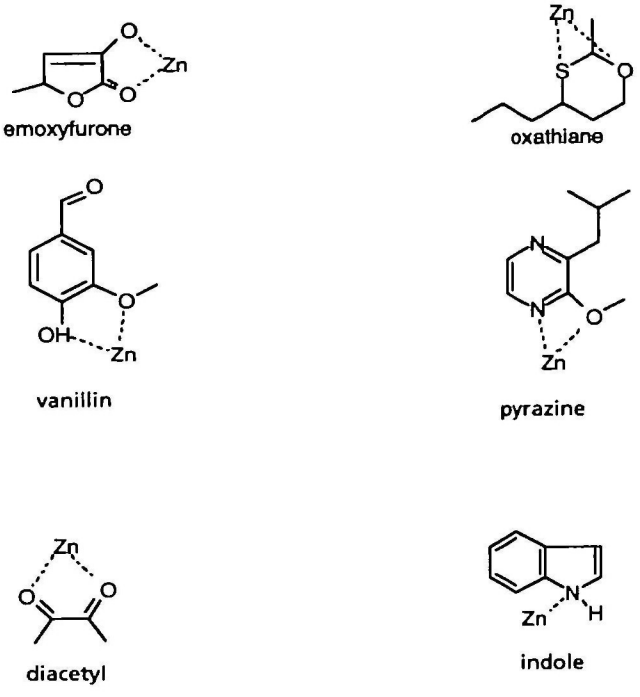

Figure 12 Six exceptionally strong odorants, showing that they share the ability to coordinate to a zinc ion. See text.

the portion of the Mopac spectra below 200 cm^{-1}. The peak centred at ~90 cm^{-1} clearly discriminates between even and odd aldehydes. The physical reason underlying both effects becomes clear when atom motions involved in the modes making up the peak are examined. These are twisting modes involving the entire hydrocarbon chain, and they have a 'wavelength' close to two C–C bonds, which explains why their amplitude will differ depending on whether the chain length is an integer multiple of the wavelength. The difference in smell, as in the vanillin–isovanillin case, appears to be due to a geometric effect on scattering by the carbonyl group.

Anomalously strong odorants: zinc binding

If an electron tunnelling mechanism is responsible for odorant transduction, one might expect there to be some relationship between atomic partial charges and the strength of an odorant. Empirically, this is the case: 'osmophoric' groups such as ketones, nitro groups, aldehydes, nitriles and ether links are all polar groups. This, however, cannot be the sole reason for differences in odorant strength. For example, vanillin is one of the strongest odorants known, whereas the closely related heliotropin is much weaker despite similar partial charges. In discussions with Dr Charles Sell (Quest International) and Prof. William Motherwell (University

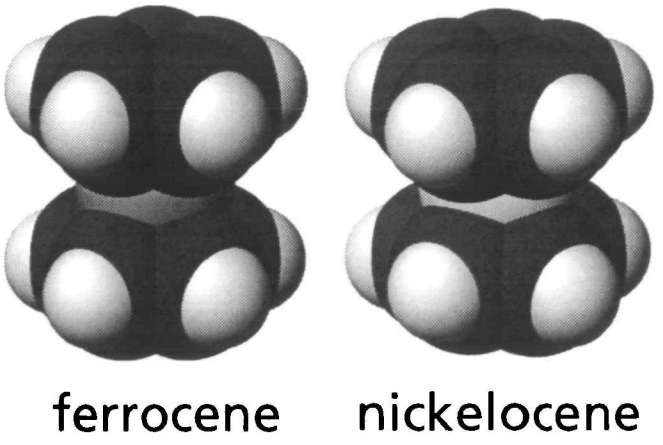

Figure 13 Space-filling models of ferrocene (left) and nickelocene (right) showing that the two molecules have virtually identical shapes (and very different odours). They also differ in the frequency of their strongest vibrational mode, involving an internal motion of the metal ion between the two rings.

College London), it was pointed out to me that the involvement of zinc in or near the active site of the olfactory receptor might account for the anomalous strengths of certain classes of odorants (see Figure 12). Thiols, nitriles and isonitriles, some of which are among the strongest odorants known, coordinate to zinc readily. Indoles bind to zinc and are very strong odorants, as are oxathianes, diketones such as diacetyl, pyrazine esters, and furanones such as emoxyfurone (3-hydroxy-4-methyl-1–5-ethyl-2,5-dihydrofuran-2-one). Binding of these molecules to the zinc ion at or near the electron tunnelling site will increase their effective concentration at the receptor and, all other things being equal, allow their detection at lower partial pressures. Conversely, if zinc binding is a general property of strong odorants, one might expect that it could be used to scavenge strong odorants from ambient air. Indeed, a solution of the zinc salt of ricinoleic acid (Grillocin) has long been used as a very effective deodorizer, and this is likely to be its mode of action. Aside from providing indirect evidence for the involvement of a metal ion in the transduction process, metal binding could be useful in fragrance design if it were possible to build into the molecule to increase odorant potency.

Molecules with near-identical shapes and different odours

Strong evidence for a tunnelling mechanism comes from the ability of electrons to tunnel through a molecule and be

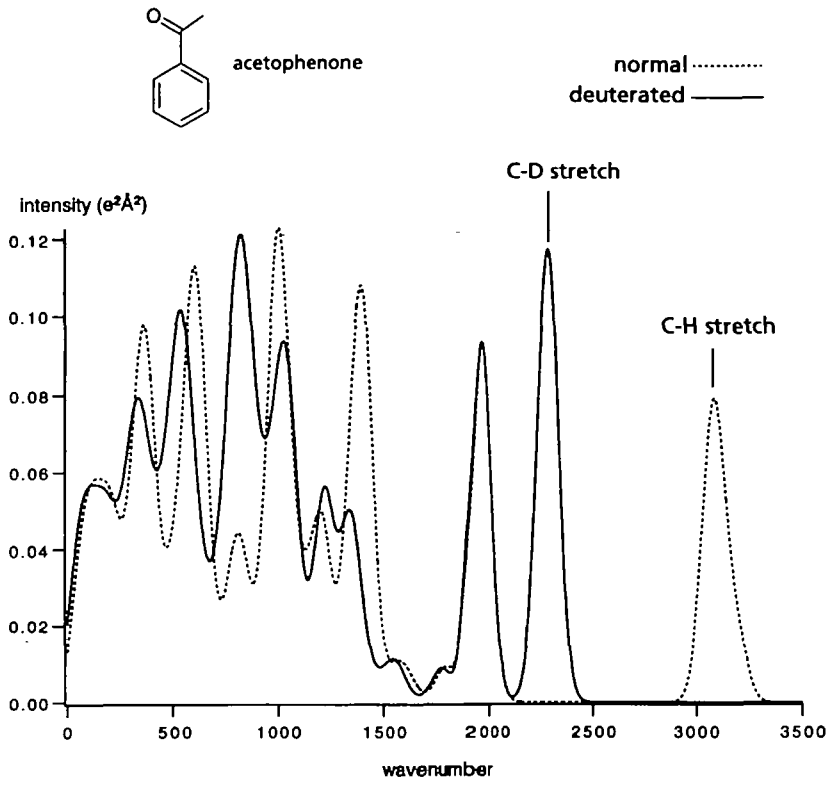

Figure 14 Structure and CHYPRE spectra of acetophenone (dotted line) and fully deuterated acetophenone-d_8. The main differences between the two spectra are the shift of C–H stretches from 3000 to 2200 cm^{-1}, a region typical of CN stretches, and the reduction in amplitude of the peak at 1500 cm^{-1}. A difference in odour character between these two molecules would be expected to exist, and does.

scattered by atoms in its interior. Complexes of cyclopentadienyl ions with iron (ferrocene) and nickel (nickelocene) are stable and very similar in size and shape, the metal atoms almost completely encased by the cyclopentadienyl rings (Figure 13). The IR spectra of ferrocene and nickelocene are virtually indistinguishable, save for the position of the intense low-frequency internal metal-ring (M-R) vibrations (Nakamoto, 1986). In ferrocene, the M-R stretch vibration is a broad peak around 478 cm^{-1}, in the aromatic C–Cl stretch region. In nickelocene, the M-R stretch lies at 355, i.e. closer to the predicted lower limit of detectability. Nickelocene has a typical cycloalkene odour, while ferrocene has a camphoraceous odour reminiscent of chloroalkanes. This correlation seems hard to explain other than by tunnelling.

Isotope replacement

The strongest test of a vibrational theory is the comparison of odours of molecules differing only in their vibrational frequencies. This can in principle be done by isotope replacement without altering molecular conformations, because 'chemical' effects of isotope replacement are small. The effects of isotope replacement on vibrational frequencies are complex and depend on the effective masses in motion in a given vibrational mode. The largest effects occur where the relative change in mass of the atom is large, and the motion involves a few atoms. For example, replacement of hydrogen (mass 1.007) by deuterium (mass 2.014) reduces CH stretch frequency from ~3000 to ~2200 cm^{-1}. Similarly, deuteration of the SH group reduces stretch frequency from 2550 to ~1800 cm^{-1}. If the vibrational theory is correct, a deuterated thiol should not have a sulphurous odour. However, the SH–SD replacement is unlikely to give definite answers, because the thiol group is weakly acidic and D–H exchange will occur very rapidly when the odorant dissolves in physiological solution. The same applies to other molecules with rapidly exchangeable protons. For example, the report by Hara (1977) that fish can distinguish between glycine and deuterated glycine is hard to interpret, because glycine contains only exchangeable protons.

Many fully deuterated molecules are commercially

available, but few are distinctive, powerful odorants. An attempt with the weak and somewhat nondescript odorant hexane revealed a small difference between its odour and that of the fully deuterated molecule. However, differences in odour between batches of nondeuterated hexane were larger still, suggesting that impurities contributed to the odour character.

A search for a stronger odorant turned up acetophenone, which has a distinctive hawthorn and orange flower smell and is available as a high-purity deuterated compound. Calculation of CHYPRE spectra of acetophenone and acetophenone-d_8 (Figure 14) suggested that odour differences should be perceptible: the peak corresponding to the CH wag modes at ~1400 cm^{-1} is absent in acetophenone-d_8 and the CH stretches are shifted into the region (~2200 cm^{-1}), which would normally indicate the presence of a nitrile (CN) group. The odours of acetophenone and acetophenone-d_8 were compared undiluted, to make sure that the weakly acidic methyl protons would not exchange with solvent hydrogen. Though both odorants have broadly similar odour profiles, the difference between them is striking: acetophenone-d_8 is fruitier and has less toluene-like character than acetophenone, and also has a much stronger bitter almonds character. The latter is particularly interesting because the spectrum of acetophenone-d_8 is closely related to that of benzonitrile, a strong bitter almond odorant.

In order to test for the possibility that impurities might be responsible for the odour difference, 0.2 µl samples of neat acetophenone and acetophenone-d_8 (Aldrich) were run through a gas chromatograph and smelled as they emerged from the GC capillary column (I am grateful to Ken Palmer at Quest international for help with the GC smelling). The deuterated acetophenone sample was found to contain only one impurity below the p.p.m. level, while the acetophenone had three p.p.m. impurities. The acetophenone-d_8 had the same odour as the bulk sample and was clearly different in odour from the acetophenone peak. In other words, two molecules with identical shapes and different vibrational spectra smell different.

ACKNOWLEDGEMENTS

I thank Geoffrey Burnstock for his generous hospitality and encouragement, and C. John Adkins, David Armstrong, Tim Arnett, Michael Marron, William Motherwell, Richard M Philpot, Guy Robert, Sir Derek Roberts, Karen Rossiter, Maurice Roucel, John W Scott, Charles Sell, Walter W Stewart, Marshall Stoneham and Igor Vodyanoy for their help. This work was funded by the US Office of Naval Research.

REFERENCES

Adkins, C.J. and Phillips, W.A. (1985) Inelastic electron tunnelling spectroscopy. *J Phys. C: Solid State Phys.*, **18**, 1313–1346.

Alpers, D.H. (1994) Zinc and deficiencies of taste and smell. *J. Am. Med. Assoc.*, **272**, 1233–1234.

Amoore, J.E. (1971) Olfactory genetics and anosmia. In Beidler, L.M. (ed.), *Handbook of Sensory Physiology*. Springer-Verlag, Berlin, vol. 4, pp. 245–256.

Arctander, S. (1994) *Perfume and Flavor Chemicals*. Allured Publishing Co., Carol Stream, IL.

Bedoukian, P.Z. (1986) *Perfumery and Flavoring Synthetics*. Allured Publishing Co., Wheaton, IL.

Beets, M.G.J. (1971) Olfactory response and molecular structure. In Beidler, L.M. (ed.), *Handbook of Sensory Physiology*. Springer-Verlag, Berlin, vol. 4, pp 257–321.

Beets, M.G.J. (1978) *Structure–Activity Relationships in Human Chemoreception*. Applied Science Publishers, London.

Buck, L. (1993) Identification and analysis of a multigene family encoding odorant receptors: implications for mechanisms underlying olfactory information processing. *Chem. Senses*, **18**, 203–208.

Buck, L. and Axel, R. (1991) A novel multigene family may encode odorant receptors- a molecular basis for odour recognition. *Cell*, **65**, 175–187.

Choi, K.N. and Barker, E.F. (1932) Infrared absorption spectrum of hydrogen cyanide. *Phys. Rev.*, **42**, 777–785.

Coleman, D.R., Berghuis, A.M., Lee, E., Linder, M.E., Gilman, A.G. and Sprang, S.R. (1994) Structures of active conformations of GIA1 and the mechanism of GTP hydrolysis. *Science*, **265**, 1405.

Dollish, F.R., Fateley, W.G. and Bentley, F.F. (1974) *Characteristic*

Raman Frequencies of Organic Compounds. J. Wiley & Sons, New York.

Dyson, G.M. (1938) The scientific basis of odour. *Chem. Ind.*, **57**, 647–651.

Erikssen, J., Seegaard, E. and Naess, K. (1975) Side-effect of thiocarbamides. *Lancet*, **7900**, 231–232.

Firestein, S., Picco, C. and Menini, A. (1993) The relation between stimulus and response in olfactory receptor cells of the tiger salamander. *J. Physiol.*, **468**, 1–10.

Fraùsto da Silva, J.J.R. and Williams, R.J.P. (1993) *The Biological Chemistry of the Elements*. Clarendon Press, Oxford.

Hanada, T., Kashiwayanagi, M. and Kurihara, K. (1994) Temperature increase abolishes ability of turtle olfactory receptors to discriminate similar odorant. *Am. J. Physiol.*, **266**, R1816–R1823.

Hansma, P.J. (ed.) (1982) *Tunnelling Spectroscopy*. Plenum Press, New York.

Hara, J. (1977) Olfactory discrimination between glycine and deuterated glycine by fish. *Experientia*, **33**, 618–619.

Henkin, R.I., Patten, B.M., Re, P.K. and Bronzert, D.A. (1975) A syndrome of acute zinc loss. Cerebellar dysfunction, mental changes, anorexia, and taste and smell dysfunction. *Arch. Neurol.*, **32**, 745–751.

Hodgkin, D.C. (1974) Varieties of insulin. The Sir Henry Dale lecture for 1974. *J. Endocrinol.*, **63**, 3P–14P.

Jaklevic, R.C. and Lambe, J. (1966) Molecular vibration spectra by electron tunnelling. *Phys. Rev. Lett.*, **17**, 1139–1140.

Jones, D.T. and Reed RR (1989) G(olf): an olfactory neuron specific-G protein involved in odorant signal transduction. *Science*, **244**, 790–795.

Klopping, H.L. (1971) Olfactory theories and the odors of small molecules. *J. Agric Food Chem.*, **19**, 999–1004.

Kuhl, P.W. (1985) A redox cycling model for the action of beta-adrenoceptor agonists. *Experientia*, **41**, 1118–1122.

Lambright, D.G., Sondek, J., Bohm, A., Skiba, N.P., Hamm, H.E. and Sigler, P.B. (1996) The 2.0 A crystal structure of a heterotrimeric G protein. *Nature*, **379**, 311–319.

Lawton, M.P., Gasser, R., Tynes, R.E., Hodgson, E. and Philpot, R.M. (1990) The flavin-containing monooxygenase enzymes expressed in rabbit liver and lung are products of related but distinctly different genes. *J. Biol. Chem.*, **265**, 5855–5861.

Nakamoto, K. (1986) *Infrared and Raman Spectra of Inorganic and Coordination Compounds*. J Wiley & Sons, New York.

Ngai, J., Dowling, M.M., Buck, L., Axel, R. and Chess, A. (1993) The family of genes encoding odorant receptors in the channel catfish. *Cell*, **72**, 657–666.

Ohloff, G. (1986) Chemistry of odor stimuli. *Experientia*, **42**, 271–279.

Raming, K., Krieger, J., Strotmann, J., Boekhoff, I., Kubick, S., Baumstark, C. and Breer, H. (1993) Cloning and expression of odorant receptors. *Nature*, **361**, 353–356.

Rasenick, M.M., Watanabe, M., Lazarevic, M.B., Hatta, S. and Hamm, H.E. (1994) Synthetic peptides as probes for G protein function. Carboxyl-terminal G alpha s peptides mimic Gs and evoke high affinity agonist binding to beta-adrenergic receptors. *J. Biol. Chem.*, **269**, 21519–21525.

Ressler, K.J., Sullivan, S.L. and Buck,L.B. (1994) A molecular dissection of spatial patterning in the olfactory system. *Curr. Opin. Neurobiol.*, **4**, 588–596.

Scrutton, N.S., Berry, A. and Perham, R.N. (1990) Redesign of the coenzyme specificity of a dehydrogenase by protein engineering. *Nature*, **343**, 38–43.

Shepherd, G.M. (1994) Discrimination of molecular signals by the olfactory receptor neuron. *Neuron*, **13**, 771–790.

Sicard, G. and Holley, A. (1984) Receptor cell responses to odorants: similarities and differences among odorants. *Brain Res.*, **292**, 283–296.

Sleigh, A.K., Phillips, W.A., Adkins, C.J. and Taylor, M.E. (1986) A quantitative analysis of the inelastic electron tunnelling spectrum of the formate ion. *J. Phys. C: Solid State Phys.*, **19**, 6645–6654.

Socrates, G. (1994) *Infrared Characteristic Group Frequencies*. J. Wiley & Sons, New York.

Weyerstahl, P. (1994) Odor and structure. *J. Prat. Chem. Zeitung*, **336**, 95–109.

Wright, R.H. (1977) Odor and molecular vibration: neural coding of olfactory information. *J. Theor. Biol.*, **64**, 473–502.

Zakarya, D., Yahiaoui, M. and Fkihtetouani, S. (1993) Structure–odor relations for bitter almond odorants. *J. Phys. Org. Chem.*, **6**, 627–633.

Zhao, H., Firestein, S. and Greer, C.A. (1994) NADPH-diaphorase localization in the olfactory system. *NeuroReport*, **6**, 149–152.

Zumkley, H., Bertram, H.P., Vetter, H., Zidek, W. and Losse, H. (1985) Zinc metabolism during captopril treatment. *Horm. Metab. Res.*, **17**, 256–258.

Received on July 31, 1996; accepted on September 30, 1996